JACS JOURNAL OF THE AMERICAN CHEMICAL SOCIETY

Article

Cite This: J. Am. Chem. Soc. 2019, 141, 4634−4643

pubs.acs.org/JACS

Spectroscopic Investigation of the Effect of Microstructure and Energetic Offset on the Nature of Interfacial Charge Transfer States in Polymer: Fullerene Blends

S. D. Dimitrov,[*,†] M. Azzouzi,[‡] J. Wu,[§] J. Yao,[‡] Y. Dong,[§] P. Shakya Tuladhar,[§] B. C. Schroeder,[∥] E. R. Bittner,[⊥] I. McCulloch,[§,#] J. Nelson,[*,‡] and J. R. Durrant[†,§]

[†]SPECIFIC, College of Engineering, Swansea University, Bay Campus, Swansea SA1 8EN, United Kingdom

[‡]Department of Physics and Centre for Plastic Electronics and [§]Department of Chemistry and Centre for Plastic Electronics, Imperial College London, London SW7 2AZ, United Kingdom

[∥]Department of Chemistry, University College, London WC1H 0AJ, United Kingdom

[⊥]Department of Chemistry, University of Houston, Houston, Texas 77204, United States

[#]Physical Sciences and Engineering Division, KAUST Solar Center (KSC), King Abdullah University of Science and Technology (KAUST), Thuwal 23955-6900, Kingdom of Saudi Arabia

Supporting Information

ABSTRACT: Despite performance improvements of organic photovoltaics, the mechanism of photoinduced electron−hole separation at organic donor−acceptor interfaces remains poorly understood. Inconclusive experimental and theoretical results have produced contradictory models for electron−hole separation in which the role of interfacial charge-transfer (CT) states is unclear, with one model identifying them as limiting separation and another as readily dissociating. Here, polymer−fullerene blends with contrasting photocurrent properties and enthalpic offsets driving separation were studied. By modifying composition, film structures were varied from consisting of molecularly mixed polymer−fullerene domains to consisting of both molecularly mixed and fullerene domains. Transient absorption spectroscopy revealed that CT state dissociation generating separated electron−hole pairs is only efficient in the high energy offset blend with fullerene domains. In all other blends (with low offset or predominantly molecularly mixed domains), nanosecond geminate electron−hole recombination is observed revealing the importance of spatially localized electron−hole pairs (bound CT states) in the electron−hole dynamics. A two-dimensional lattice exciton model was used to simulate the excited state spectrum of a model system as a function of microstructure and energy offset. The results could reproduce the main features of experimental electroluminescence spectra indicating that electron−hole pairs become less bound and more spatially separated upon increasing energy offset and fullerene domain density. Differences between electroluminescence and photoluminescence spectra could be explained by CT photoluminescence being dominated by more-bound states, reflecting geminate recombination processes, while CT electroluminescence preferentially probes less-bound CT states that escape geminate recombination. These results suggest that apparently contradictory studies on electron−hole separation can be explained by the presence of both bound and unbound CT states in the same film, as a result of a range of interface structures.

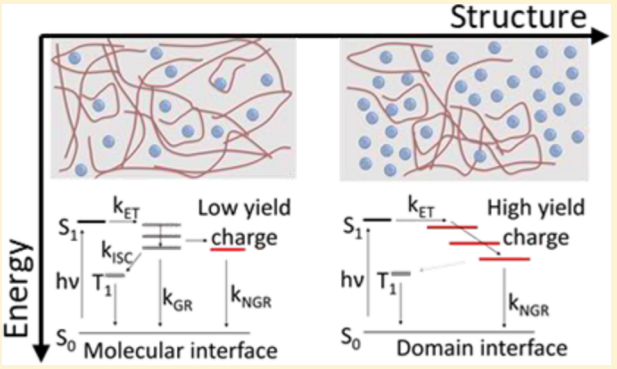

INTRODUCTION

Recent technological advances in organic photovoltaics (OPV) have resulted in the development of devices with power conversion efficiencies of >17%.[1] An unresolved scientific challenge for this technology is understanding−and controlling−the mechanism of photoinduced electron−hole (e−h) separation. Specifically, the extent to which Coulombic interactions between the electron and hole directly after exciton dissociation at a donor:acceptor (D:A) interface limit photocurrent generation has remained controversial,[2] because of inconclusive evidence from experimental and theoretical studies producing contradictory e−h separation models.[3−8] There is extensive evidence from transient absorption and photoluminescence (PL) spectroscopic studies for the existence of photogenerated e−h pairs that are spatially localized and subject to stronger Coulombic binding interaction which, once formed, can limit photocurrent

Received: October 24, 2018
Published: February 26, 2019

DOI: 10.1021/jacs.8b11484
J. Am. Chem. Soc. 2019, 141, 4634−4643

generation.[4,9−13] We refer herein to such states as bound interfacial charge-transfer (CT) states. The presence of such CT states is evidenced by electric-field-dependent studies and pump−push transient studies indicating extra energy can assist in dissociating these intermediate CT states into separated e−h pairs.[14−18] Some, but not all, transient studies have shown that the yield of separated e−h pairs increases with an increasing enthalpic offset between the photoexcited donor (or acceptor) singlet state and the nominal D:A charge separated state in series of chemically similar blends, suggesting that an increased offset may help photogenerated e−h pairs avoid prompt recombination at the D:A interface by overcoming their Coulombic binding energy.[19−21] Furthermore, photoluminescence studies probing sub-band-gap CT transitions have demonstrated the existence of CT states with different degrees of an e−h pair separation radius, and hence, binding energy.[22] However, this evidence for Coulombically bound interfacial CT states contrasts with studies which show that internal quantum efficiency in studied devices remains almost invariant down to energies far into the tail of CT states,[5,6] assayed with sub-band-gap CT electroluminescence (EL) measurements, suggesting that photoexcitation of sub-band-gap transitions can result directly in efficient photocurrent generation. Since the CT states readily generate photocurrent, it could be concluded that they are only weakly Coulombically bound.[5,6,8,23,24] These observations led to the view that the generation of separated electrons and holes proceeds through thermally relaxed CT states which are dissociated relatively easily at room temperature. This is supported by recent studies reporting low activation energies of $\sim kT$ at room temperature for the separation of CT states into free e−h pairs.[25] To date, these two bodies of experimental work have remained largely distinct, without a clear resolution of their apparently contradictory conclusions. Part of the difficulty in reconciling the evidence, from different studies, for bound and unbound interfacial CT states lies in the fact that the different studies typically address different materials systems of different microstructure as well as being based on different experimental techniques.

Theoretical studies of the excited states of D:A blends show that the interface can, in general, support a range of states of different energy and of different degree of excitonic, CT, or charge separated character.[26] The particular spectrum and the extent to which the different states are sampled will also be a function of the blend microstructure. D:A polymer: fullerene blends tend to contain mixed regions where acceptor molecules are dispersed within amorphous polymer domains as well as pure (possibly crystalline) domains of both acceptor and donor.[27−32] The volume fractions adopted by each domain will depend on the tendency of each component to crystallize and the miscibilities of each component in each other as well as on the composition ratio. We therefore expect typical OPV blends to include both bound and unbound interfacial CT states, with the more mixed domains supporting more strongly bound, CT type states while interfaces between more extended domains support relatively unbound CT states. The local microstructure is already known to affect charge separation efficiency with the presence of pure domains of at least one component correlating with increased charge separated yields and suppression of the geminate recombination losses from bound CT states.[5,13,18,30,33,34]

The apparent disagreement between different studies may thus be resolved by recognizing that different experimental techniques probe different subsets of these interfacial states and by the fact that different studied blends will express these different types of states to different degree. Indeed, previous studies of sub-band-gap CT state PL and EL have assigned the different emission spectra and properties to two different classes of CT states within the same blend.[15]

In this study, we use a range of spectroscopic techniques to probe the impact of interfacial energetics and blend microstructure on the balance between free and bound charge pair generation, using as model systems high offset and a low offset polymer:fullerene blends, each of varying composition. The relative importance of tightly bound CT states is quantified through observation of (geminate) charge recombination on the nanosecond time scale and is found to depend on both blend microstructure and energetics. In particular, while phase segregation can assist e−h separation (i.e., suppress the relative density of the tightly bound states) in the high offset system, it fails in the low offset case. We use a lattice exciton model of the states in different systems to rationalize this result in terms of the relative fractions of more and less tightly bound CT states in the different systems. The study provides a picture of the relationship between microstructure, energetics, state configuration, and spectroscopy which may help to reconcile previous experimental observations of both bound and unbound interfacial CT states in bulk-heterojunction OPV.

RESULTS

The first polymer:fullerene blend studied herein is poly[*N*-9′-heptadecanyl-2,7-carbazole-*alt*-5,5-(4′,7′-di-2-thienyl-2′,1′,3′-benzothiadiazole)]:phenyl-C61-butyric acid methyl ester (PCDTBT:PCBM) which is a high LUMO−LUMO energy offset system (0.73 eV)[35] based on an amorphous polymer and which exhibits high photocurrent generation yields for blends of 1:4 and 1:2 by weight. Four PCDTBT:PCBM blend films, with 4:1, 2:1, 1:2, and 1:4 weight ratios, were spin-coated onto glass substrates for the spectroscopic analysis. The PL from PCDTBT singlet excitons (Figure S1) is strongly quenched by PCBM in all four blends, confirming that electron transfer is highly efficient in this system and indicating that PCBM mixes well into the PCDTBT polymer at a molecular scale.[36] The PL from PCBM excitons is strongly quenched only in the 4:1 and 2:1 blends, but not in the 1:2 and 1:4 blends, assigned in the high PCBM content blends to pure PCBM domain formation on the tens of nanometer length scale limiting the yield of excitons undergoing hole transfer.[37] These PL results reflect the structural differences between the four PCDTBT:PCBM films and are consistent with direct morphological studies reported in the literature on these and analogous blends.[27−32] We consider that two main phases are present in these blend films: an intermixed polymer:fullerene phase in which the molecular D:A interface is dominant and a pure fullerene phase. The intermixed phase dominates the 4:1 and 2:1 blends, while both phases should be present in the 1:2 and 1:4 blends.

Transient absorption spectroscopy (TAS) was used to study the photogenerated charge dynamics on the picosecond and nanosecond time scales as a function of blend composition and excitation density. Figure 1c,d present the PCDTBT ground-state bleach dynamics in the 4:1 and 1:4 PCDTBT:PCBM blend films. PCDTBT exciton separation in both films is known to be ultrafast and completed within 1 ps (see also the Supporting Information for confirmation of this from TAS and PL quenching data for the films studied herein).[36] Therefore, on the time scales studied, exciton separation is complete;

DOI: 10.1021/jacs.8b11484
J. Am. Chem. Soc. 2019, 141, 4634−4643

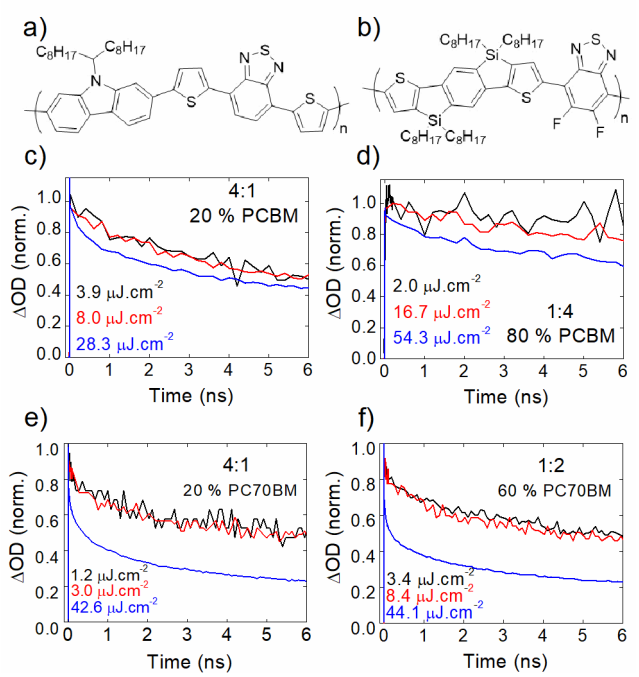

Figure 1. Polymer chemical structures of (a) PCDTBT and (b) SiIDT-2FBT and (c, d) transient absorption bleach dynamics of 4:1 and 1:4 PCDTBT/PCBM blends (recorded at 3 excitation intensities with 510 nm excitation pulses and probed at 590 nm) and (e, f) polaron absorption decay dynamics of 4:1 and 1:2 SiIDT-2FBT/PC70BM blends recorded at 3 excitation intensities with 635 nm pulses and probed at 980 nm.

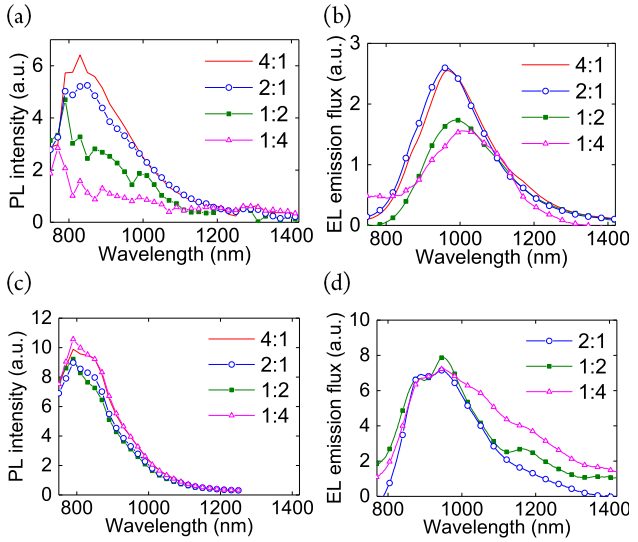

Figure 2. Sub-band-gap photoluminescence and electroluminescence spectra from CT transitions of (a, b) PCDTBT:PCBM and (c, d) SiIDT-2FBT:PC70BM blends recorded as a function of composition. Excitation wavelength for PCDTBT:PCBM PL measurements was 560 nm and for SiIDT-2FBT:PCBM measurements was 635 nm.

these data therefore provide a direct assay of the PCDTBT hole decay dynamics, probing the density of both bound and unbound hole polarons. The bleach decay dynamics are clearly blend composition dependent, indicating differences in the hole dynamics of these structurally different films. The 4:1 blend, consisting mainly of an intermixed phase, has a strong nanosecond signal decay of >50% by 6 ns, which is intensity independent at low excitation fluences. Such behavior is typical for geminate recombination processes of spatially correlated e−h pairs (i.e., bound CT states) and reveals their dominance in this film structure. Similar geminate losses are not detected for the 1:4 film, which shows negligible nanosecond signal decay for the lowest used excitation intensity. Instead, this film only displays significant nanosecond decay dynamics at high laser excitation intensities, indicating the dominance of nongeminate recombination of dissociated polarons at moderate to high excitation fluence in this high fullerene content blend film. The suppression of geminate recombination with higher fullerene content blends is known to correlate with higher photocurrent generation and has been assigned to the presence of pure fullerene domains facilitating the dissociation of photogenerated charges.[30,33,34,38] Further data were collected for 2:1 and 1:2 blend ratios; the correlation between geminate recombination losses and blend composition is summarized in Figure 4 below.

Charge transfer photoluminescence and electroluminescence data from 4:1, 2:1, 1:2, and 1:4 PCDTBT:PCBM blend films are presented in Figure 2a,b. The CT state PL is observed with a peak at ∼820 nm, clearly red-shifted from the PCDTBT exciton emission at 705 nm, consistent with its assignment to interfacial CT state emission.[39] The composition dependence shown in Figure 2a reveals a clear trend of suppressed CT PL from the films with a higher fullerene content, which correlates with the suppression of geminate CT state recombination observed in our transient absorption data. In agreement with this are the decay lifetimes of the CT PL emitted by the 4:1 and 1:4 films which have time constants (τ) of 1.27 ns (with an exponent b = 0.59) and 0.13 ns (with b = 0.47), correspondingly, as determined by fitting time-correlated single photon counting (TCSPC) data with a stretched exponential function ($\exp(-t/\tau)^b$) (Figure S2). The time constant of the polymer rich film is similar to the 3.2 ns time-constant of geminate recombination in the same film estimated from exponential fitting of the ground-state bleach recovery dynamics of this blend film (Figures 1 and S3). These data therefore indicate that the CT state photoluminescence emitted from the polymer-rich PCDTBT:PCBM blend films results from the same population of e−h pairs that dominate the geminate recombination kinetics and that recombination by these bound CT states is only dominant in films whose morphology is dominated by a molecularly intermixed PCDTBT:PCBM phase, without significant nanoscale phase segregation into pure domains. Supporting this conclusion, the suppression of geminate recombination in blends with a high fullerene content also results in suppression of CT PL intensity.

We also recorded the CT state electroluminescence from devices made from the four PCDTBT:PCBM blends (Figure 2b) which agrees with published data.[39] This electrically generated CT state EL is clearly red-shifted from the CT state PL generated by photoexcitation. We note that the same shift of EL relative to PL is observed when PL is measured on the same PCDTBT:PCBM device as the EL.[40] The CT state EL also red-shifts with the addition of extra PCBM and is red-shifted from the excitonic neat polymer EL.[16,39] An analogous composition-dependent CT state EL red shift has been commonly observed,[15] which has been suggested to be caused by the stabilization of the PCBM's LUMO upon aggregation, as well as a rise of the film's dielectric constant.[41] These data clearly indicate that PL and EL sample the distribution of CT

DOI: 10.1021/jacs.8b11484
J. Am. Chem. Soc. 2019, 141, 4634−4643

states in these blends differently. The same behavior has been observed previously,[17] for example for AnE PV (anthracene-containing poly(*p*-phenylene ethynylene)-*alt*-poly(*p*-phenylenevinylene)) copolymers[42] and as discussed further below.

Low excitation density TAS measurements on the nano- and microsecond time scales (Figure 3a,b) in the presence and

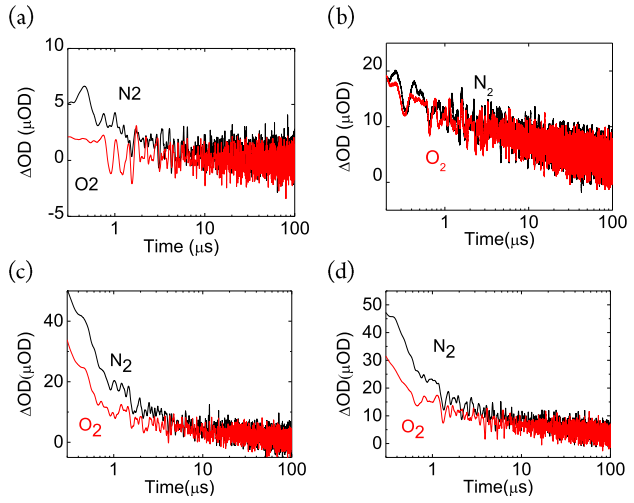

Figure 3. Nanosecond TAS of (a, b) PCDTBT:PCBM 4:1 (a) and 1:4 (b) blend films probed at 1060 nm and (c, d) SiIDT-2FBT:PC70BM 4:1 (c) and 1:2 (d) blend films probed at 1100 nm. The data were recorded with excitation fluence of 0.6 μJ/cm^2 and wavelength at the polymer absorption and under N_2 (black) and O_2 (red) atmosphere. Quenching of the signal under O_2 is an indicator for the presence of photogenerated triplet states in the films.

absence of oxygen indicate that the PCDTBT:PCBM blends form both long-lived polaron and triplet state signals as photoproducts. The presence of triplets is inferred from the shortening of the lifetime of the transient absorption signal under oxygen-rich environment compared to that under nitrogen-rich environment, caused by triplet to molecular oxygen energy transfer and the change of decay dynamics from mostly exponential (characteristic of triplet dynamics) to purely power law (characteristic of charges), as shown in Figure S4. However, while photoexcitation of the 4:1 blend yields mainly long-lived triplets, the 1:4 blend has predominantly long-lived polarons. The observation of triplets in the 4:1 blend can be assigned to intersystem crossing within bound CT states and subsequent geminate recombination to the polymer triplet or nongeminate e−h recombination on the nanosecond time scale.[16,43] The reduction in triplet yield with higher PCBM content is consistent with this assignment and with the suppression of geminate recombination from bound CT states at high PCBM content discussed above.

The second polymer:fullerene blend studied is silaindacenodithiophene-5,6-difluorobenzo[*c*][1,2,5]thiadiazole:phenyl-C71-butyric acid methyl ester (SiIDT-2FBT:PC70BM) which is based on a relatively crystalline polymer, possesses a low LUMO−LUMO offset (0.10−0.14 eV)[16,44] and shows poor e−h separation properties limited by geminate recombination at all compositions. Exciton emission quenching in this blend is also very high, ∼95%, showing efficient mixing of fullerenes into the polymer and separation of excitons at the polymer:fullerene interface in all compositions. This is further confirmed by subpicosecond polaron formation as inferred from the data in Figure S5 and reported in ref 16. Figure 1e,f presents the polaron absorption signal decay for the 4:1 and 1:2 blends with this polymer, recorded as a function of excitation intensity. Nearly identical signal decays are observed for both compositions, undergoing 45% intensity independent signal loss by 6 ns, assigned to geminate CT state recombination. Sub-band-gap CT PL and EL experiments shown in Figure 2c,d also reveal weak dependence of the spectra and emission peak position on composition for the SiIDT-2FBT:PC70BM films, in contrast to PCDTBT:PCBM. A similar composition independence is also seen in the triplet state dynamics in Figure 3c,d. These results demonstrate clearly that SiIDT-2FBT:PC70BM blends exhibit different behavior to the PCDTBT:PCBM blends at high fullerene content. These SiIDT-2FBT:PC70BM blends exhibit composition independent geminate recombination, CT state PL and triplet yields, consistent with the suggestion above that both CT state PL and transient triplet yields measured at low excitation densities derive from the geminate recombination of bound CT states.

DISCUSSION

Figure 4 summarizes the results described above for both PCDTBT:PCBM and SiIDT-2FBT:PC70BM polymer:fullerene blend systems by plotting their (i) geminate recombination loss at 6 ns estimated with TAS, (ii) amplitude of CT PL, and (iii) photogenerated triplet yields estimates at 0.2 μs, all as a function of blend composition. Focusing first on PCDTBT:PCBM, the TAS estimates of the geminate loss in this system are in line with published time-resolved spectroscopy work by Laquai et al. showing 11% losses in 1:2 PCDTBT:PCBM and the 20% loss at max power point estimated by Stolterfoht et al. in a complete device also of composition 1:2 PCDTBT:PCBM.[45,46] Geminate recombination has also been demonstrated for several other polymer:fullerene systems.[34,38,47,48] We find that the magnitude of the geminate recombination loss, as plotted in Figure 4, is strongly dependent on the fullerene content and consistent with the role of fullerene aggregation in the suppression of the nanosecond geminate recombination processes. The loss of charges via recombination on the nanosecond time scale is expected to be faster than the extraction of charges by the electrodes in PCDTBT:PCBM devices.[33,49] Our data are also

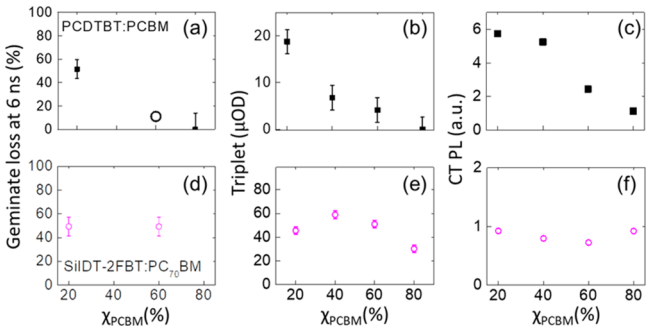

Figure 4. Summary graphs of extracted geminate recombination losses estimated from polaron and bleach absorption in TAS at 6 ns (a, d), polymer triplet amplitude estimated with TAS at 0.2 μs (b, e), and CT PL amplitude (c, f) for PCDTBT:PCBM (top 3 graphs: a−c) and SiIDT-2FBT:PC70BM (bottom 3 graphs: d−f) films, as a function of composition. χ_{PCBM} is the weight percentage of fullerene in the blend films.

DOI: 10.1021/jacs.8b11484
J. Am. Chem. Soc. 2019, 141, 4634−4643

consistent with reports in the literature of film microstructure playing a key role in the charge separation dynamics on the nanosecond time scale in other blends with high energy offsets and ultrafast exciton separation.[33,34]

Figure 4b also demonstrates that the changes in film microstructure that result from higher PCBM content strongly reduce the yield of photogenerated triplet excitons in PCDTBT:PCBM, which qualitatively follow the reduction in geminate CT recombination losses. This is consistent with the triplet excitons being generated via a spin flip from the bound CT state that also results in geminate e−h recombination, as demonstrated recently for SiIDT-2FBT:PC70BM.[16] This geminate triplet generation process differs from the bimolecular recombination of spin-uncorrelated charges[43] also observed in the current study but at higher excitation intensities (Figure S6).

The sub-band-gap emission from the PCDTBT:PCBM blends exhibits well-resolved CT PL which, as seen in Figure 4c, decreases in amplitude with the addition of excess fullerene. The similar time-constants for CT PL and TAS in the 4:1 blend, indicate that the CT PL probes the same geminate e−h recombination process as TAS. As such, the decay of CT PL in these blends reflects the geminate recombination of charges within molecularly intermixed PCDTBT:PCBM domains.

The effect of increasing fullerene content on the charge-carrier dynamics in SiIDT-2FBT:PC70BM blends appears to be quite different from that in PCDTBT:PCBM blends, as indicated by the bottom panels of Figure 4. The fraction of geminate CT state recombination, as quantified by the lifetime of the charged states probed by TAS, by the intensity of CT PL, and by the incidence of triplet states, appears to be nearly insensitive to the fullerene content. While this behavior could, in principle, be explained by a much higher miscibility of PC70BM in the SiIDT-2FBT polymer than in PCDTBT, this is unlikely since SiIDT-2FBT is a relatively crystalline polymer which is likely to result in an even lower miscibility of PCBM in that material as in PCDTBT. For reference, typical miscibility of PCBM into conjugated amorphous polymers lies at around 20% for more amorphous blends (such as regiorandom P3HT:PCBM and PCDTBT:PCBM) and 8% for MDMO-PPV:PCBM.[50−53] The insensitivity to PCBM content of the EL emission spectrum from this system is another indicator of the different impact of PCBM loading on the nature of the CT excited states.

We remark briefly on the comparison of CT state PL and EL spectra. In comparison with CT PL, the CT EL from the PCDTBT:PCBM blends (Figure 2) is red-shifted from CT PL by at least >0.1 eV and shows a distinct redshift in peak emission energy as PCBM content increases, both as previously reported for several other systems,[15,17,41] (although recently reported EL and PL spectra of PCPDTBT:PCBM devices overlapped in energy suggesting material specific behavior).[54] The results presented here can be explained by the fact that in CT EL injected carriers populate the lowest available energy interfacial CT states in the density of states (DoS) of the conduction and valence bands and that the electron states will tend to shift to lower energy with increasing PCBM content as PCBM domains enlarge. In contrast, in CT PL, CT states are generated at the D:A interface by photoexcitation and may recombine rapidly (on the ns time scale) before the carriers have time to relax during transport into the lowest energy states in the DoS. When the CT PL is driven by photoexcitation of the polymer, its spectrum reflects the energies of CT states primarily at the interfaces adjacent to the polymer and will tend to be dominated by molecularly mixed polymer:PCBM domains at low PCBM content, with a larger contribution from aggregated PCBM domains in PCBM rich blends. As a result, we expect CT EL to be red-shifted relative to CT PL and to red-shift further with increasing PCBM content.

It now remains to explain the different impacts of increasing fullerene content on the nature of charge-carrier recombination in the two types of blends. Given that in both cases fullerene aggregation will occur once the fullerene content exceeds the miscibility limit, the qualitative trend in type of interface with fullerene content will be similar (i.e., tending from interfaces solely with small PCBM domains or individual molecules at low PCBM content to interfaces with both small and large domains at high content). The reason for different excited state behavior must therefore lie elsewhere than in radical differences in the range of microstructures probed in the two cases. A plausible reason is the smaller offset between donor singlet energy and nominal CT state energy for the SiIDT-2FBT:PC70BM blend than for PCDTBT:PCBM and the effect of this offset on the nature of the interfacial states. To explore this effect, we implement a two-dimensional lattice exciton model to simulate the excited state spectrum of a polymer:-fullerene blend system as a function of both microstructure and LUMO energy offset.[26,55−57] We model the microstructure as a combination of a "mixed" phase containing PCBM molecules and small PCBM domains mixed into polymer, and a "clustered" phase consisting of a large fullerene cluster, with increasing fraction of clustered phase as the volume fraction of PCBM increases (Figure 5a,b). We assign a lower HOMO−LUMO gap to the polymer then to the fullerene, and we use large (0.7 eV) and small (0.1 eV) offsets in the LUMO between the two components to represent the large and small offset systems. We then calculate the set of excited states for each system, distinguishing states in terms of their CT versus excitonic character, as well as their energy, and calculate the emission spectrum that would be expected from that distribution of excited states in an EL measurement. The character (excitonic or CT) of the excited states is defined according to how much charge is transferred from the donor to acceptor; states with <0.1 electronic charge (e) transferred are defined to have an excitonic character (blue), states with 0.1−0.9 e transferred are called mixed states (green), and states with >0.9 e transferred are called CT states (red). The lowest gap pure component (the donor) starts to absorb only above 2.2 eV in this model (Figure S8e). The modeled microstructures and energy levels of the systems studied are shown in Figures 5 and S8, and the model, which is adapted from ref 26, is described in the Supporting Information.

The simulated, normalized electroluminescence spectra for the low-offset and high-offset systems (Figure 5c,d) show the same behavior as that observed experimentally, namely, that the luminescence redshifts with increasing fullerene content only in the case of the high offset system. In the high offset case, the lowest energy excited states that dominate the EL have CT character for all compositions. These low-energy CT-like states tend to reduce in energy slightly with increasing fullerene content because fullerene aggregation pushes down the energy of the lowest fullerene electron states, and hence the lowest CT states, thus leading to the redshift in emission peak. In the low-offset case, the lowest energy donor exciton and CT state are known to be close in energy and tend to mix;

DOI: 10.1021/jacs.8b11484
J. Am. Chem. Soc. 2019, 141, 4634−4643

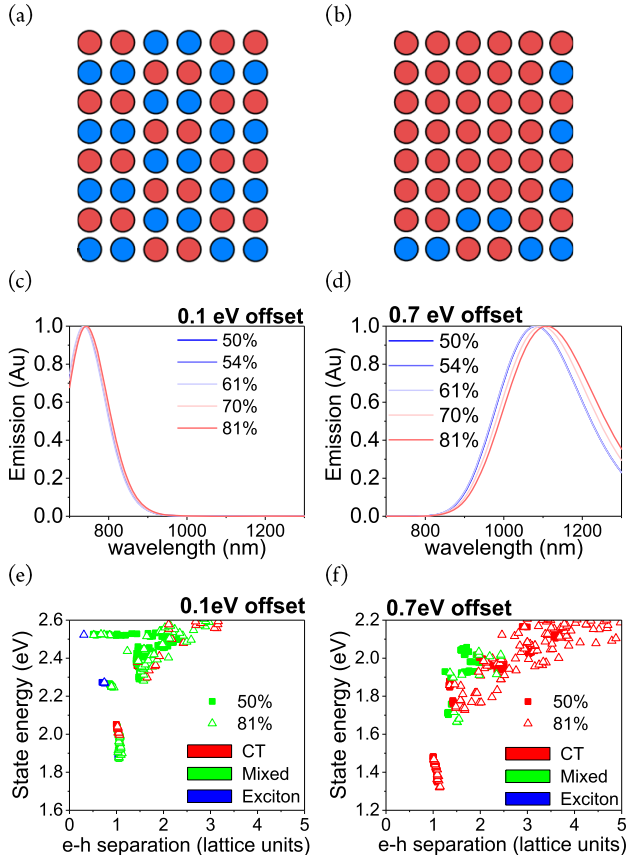

Figure 5. (a, b) Two-dimensional microstructure where blue and red mark polymer and fullerene domains, respectively, for the limit of (a) completely mixed microstructure (50 vol % acceptor) and (b) structure with high fullerene content, mainly present as a large cluster. (c, d) Simulated electroluminescence spectra as a function of acceptor volume fraction in the case of the LUMO energy offset of (c) 0.1 and (d) 0.7 eV. The simulated emission spectrum red-shifts with increasing fullerene content only in the case of the large LUMO energy offset. (e, f) Energies of the lowest energy excited states plotted as a function of mean electron−hole separation, in lattice units, for systems with different fullerene content representing more mixed (50% vol) and more clustered (81% vol) microstructure and LUMO energy offset of (e) 0.1 eV and (f) 0.7 eV. States are distinguished according to how much charge is transferred from donor to acceptor as follows: excitonic: less than 0.1 *e* transferred (blue); mixed: between 0.1 and 0.9 *e* transferred (green); and charge transfer (CT): over 0.9 *e* transferred (red).

as a result, the lowest excited states calculated by the model are excitonic or mixed in character for both the most mixed microstructure (50 vol % of acceptor) and the most clustered structure (81 vol % of acceptor) (Figure 5e). Because of the strong state mixing, the emission in the low offset system is not yet dominated by states with a pure CT character (>0.9 *e* transfer) which would be expected to enable charge separation. Moreover, by changing the offset in the model to 0.2 and 0.3 eV (see Figure S8), we observe that the lowest excited states become progressively more CT-like and less mixed in character.

The different character of the excited states of the low- and high-LUMO-offset systems help us to understand the impact of the nature of the excited states on charge separation. In the low-offset case, many of the excited states are of mixed rather than CT character, and some are excitonic. Mixed character implies incomplete separation of electron and hole into the different domains and a lower probability of charge separation. Such states may be expected to undergo geminate recombination. In the high-offset case, the majority of the low energy excited states are CT-like in character for all compositions, indicating efficient charge pair separation between donor and acceptor components. Thus, the model suggests that the body of low energy excited states formed at the interface in a high-LUMO-offset system would favor electron−hole separation relative to geminate recombination. The model also suggests that the ratio of CT to mixed character states from the complete excited state manifold is higher in the clustered structure than in the fully mixed structure, which suggests the existence of a greater density (probability) of e−h separation pathways in the clustered system. This is consistent with the experimental observation of lower geminate losses in the optimized high offset PCDTBT:PCBM (1:4) films. Furthermore, regarding the effect of PCBM on the high offset system, the model provides evidence of a slightly greater spatial separation in the clustered system, in agreement with results published by Savoie et al.[58] When such states are relatively extended spatially, the Coulombic binding between electron and hole will be weak, suggesting relative ease of charge separation for the clustered system, as seen in Figure 1 and previously reported for similar systems.[33,34]

Focusing on the body of states calculated for the low-LUMO-offset case, this system features more mixed, less CT-like states which would be likely to result in geminate recombination and can be expected to be susceptible to the application of external electric fields as previously reported.[16,34,38,54] This is consistent with the observation that often very low offset polymer:fullerene systems do not support efficient electron−hole separation.[4,9−18]

Model for Charge Separation. Figure 6 depicts a simplified model for e−h separation dynamics based upon the experimental and modeling results for the contrasting PCDTBT:PCBM and SiIDT-2FBT:PC70BM blends. The structure of the films consists of (1) molecular interfaces within a molecularly intermixed polymer:fullerene phase (which dominate in the polymer rich blends) and (2) intermixed and pure domain interfaces (which dominate in the more fullerene rich blends). After photoexcitation of the polymer, exciton dissociation in all blends is completed within hundreds of femtoseconds either at interfaces in the intermixed phase or, in the case of fullerene rich blends, at interfaces with fullerene domains. Upon exciton dissociation, CT states are populated which then show distinctly different nanosecond dynamics dependent upon the energy offset and structure of the film. In the case of the higher offset PCDTBT:PCBM system, the interfacial CT states decay by geminate recombination on the nanosecond time scale in the polymer-rich films where the intermixed phase dominates, while CT states dissociate leading to efficient e−h separation when fullerene domains dominate the films. We propose that this improvement in e−h separation efficiency with fullerene aggregation results from the population of more spatially delocalized CT states at the interfaces with fullerene domains and the greater number of such states that are accessible at room temperature (Figure 5).[30,58,59] This improved separation efficiency should also be facilitated by enhanced electron mobility in the larger fullerene domains.[60] In the case of the lower offset system, polymer exciton dissociation is also ultrafast and efficient, but nanosecond geminate recombination

DOI: 10.1021/jacs.8b11484
J. Am. Chem. Soc. 2019, 141, 4634−4643

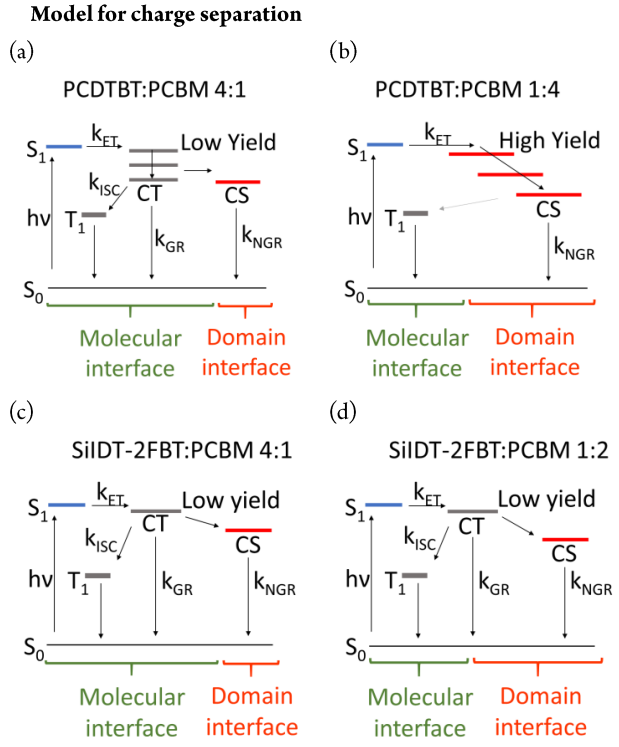

Figure 6. Model for charge photogeneration depicting the e−h separation dynamics at molecular interfaces within molecularly intermixed domains and at interfaces between pure and intermixed domains. k_{ET} refers to the rate of polymer exciton dissociation by electron transfer; k_{ISC} is rate of T_1 population from CT states; k_{GR} is rate of geminate recombination; k_{NGR} is rate of nongeminate recombination; S_1 refers to polymer singlet excitons; S_0 is ground state, T_1 is polymer triplets; CT is charge transfer states; CS are separated e−h pairs.

occurs even in the presence of fullerene domains, because the majority of low-lying excited states have excitonic or partial charge-transfer character and so are unable to dissociate readily into separate charges. The low efficiency of charge separation allows the states to undergo intersystem crossing to generate polymer triplets.

CONCLUSION

The role of interfacial CT states in limiting photocurrent generation in OPV has remained controversial because of different experimental evidence supporting contradictory models for charge separation. In this study, we use a combination of optical spectroscopy techniques and theoretical modeling based on a two-dimensional lattice exciton model to develop deeper understanding of the electron−hole separation dynamics in PCDTBT:PCBM and SiIDT-2FBT:PC70BM films with different structured and interfacial energetics. By varying the polymer:fullerene composition, we change the films from consisting of a molecularly mixed polymer:fullerene phase only to films with mixed and pure PCBM phases. Our spectroscopic results for PCDTBT:PCBM indicate an ultrafast electron transfer process populating CT states in the intermixed phase; these states are found to escape geminate recombination on the nanosecond time scale only in the presence of fullerene domains. SiIDT-2FBT:PC70BM also shows ultrafast electron transfer but behaves completely differently displaying nanosecond geminate CT state recombination for all film structures studied. This is explained within our model by the higher proportion of interfacial states with an excitonic or partial CT character in the low-offset system. A number of other factors, not included in the model, such as differences in the degree of disorder in electronic and excitonic site energies between the materials, and variations in the density of isoenergetic CT and triplet states that could affect the rate of back-electron transfer to the triplets would be interesting topics for further study. Our results provide insight into the dynamics of photogenerated charges in polymer:-fullerene blends with varied enthalpic energy offsets and structures. They also show differences between CT transitions probed by EL and PL spectroscopy indicating that EL and PL measurements probe CT states with distinctly different roles in the e−h separation dynamics and sample different types of interface in the studied films. CT transitions detected with PL techniques reflect e−h pair dynamics at all interfaces including molecular interfaces within intermixed domains. In contrast, the CT EL technique only probes CT states formed at electronically accessible interfaces such as those between intermixed and pure domains, where CT states tend to be more weakly bound and can dissociate more readily into separated e−h pairs.

EXPERIMENTAL SECTION

Materials. PCDTBT:PCBM films were spin-coated at 2000 rpm for 1 min from 25 g/L chlorobenzene solutions of PCDTBT and PCBM with varied weight ratios of 4:1, 2:1, 1:2, and 1:4 onto glass slides. PCDTBT was used as purchased from Ossila Ltd. and PCBM as purchased from Sigma-Aldrich. Slides were cleaned with soap water, water, acetone, methanol, and isopropanol under sonication. SiIDT-2FBT: PC70BM films were spin-coated following a similar procedure and from 25 g/L *o*-dichlorobenzene solutions with 4:1, 2:1, 1:2, and 1:4 weight ratios.

Fluorescence and Electroluminescence Measurements. Fluorescence from films was recorded in ambient air using Fluorolog-2 equipped with visible and NIR monochromators coupled to a Silicon and liquid Nitrogen cooled InGaAs photodiodes. Electroluminescence spectra of complete devices of the SiIDT-2FBT:PC70BM and PCDTBT:PCBM blends prepared from solutions used for spectroscopic studies were measured with a spectrograph (Shamrock 303) with a InGaAs photodiode array (iDUS) cooled to −90 °C at 178 mA/cm^2 current density (device area was 0.045 cm^2).

Time-Correlated Single Photon Counting. TCSPC measurements of fluorescence lifetime were conducted using a Delta Flex system (Horiba Scientific). The excitation was a 404 nm laser diode (Horiba scientific) with a 1 MHz repetition rate.

Transient Absorption Spectroscopy. TAS on the nanosecond and microsecond time scale was carried out with excitation pulses generated by a tunable optical parametric oscillator (Opolette 355) and probe light generated by thermally stabilized tungsten lamp (Bentham, IL 1). The excitation light intensity was controlled with dichroic neutral density filters and the probe wavelength selected using a single-grating monochromator. The probe was detected by Si or InGaAs photodiodes (Hamamatsu Photonics) which were amplified by Costronics Electronics preamplifier and amplifier electronics including a filtering circuit. The amplifier was connected to an Oscilloscope (Tektronics, TDS220) synchronized with a trigger pulse from a Si photodiode directly pumped by the optical parametric oscillator. The sample was placed in a quartz cuvette and kept under constant supply of nitrogen or oxygen to record kinetics.

Femtosecond TAS was conducted using a HELIOS transient absorption spectrometer (Ultrafast systems) with a 6 ns delay stage seeded by a 1 kHz, 800 nm, 100 fs Solstice Ti:sapphire regenerative amplifier (Newport Ltd.). The pump pulses were generated by a TOPAS optical parametric amplifier (Light conversion). All measure-

DOI: 10.1021/jacs.8b11484
J. Am. Chem. Soc. 2019, 141, 4634−4643

ments were conducted with samples placed in a quartz cuvette kept under dry nitrogen atmosphere.

■ ASSOCIATED CONTENT

Supporting Information

The Supporting Information is available free of charge on the ACS Publications website at DOI: 10.1021/jacs.8b11484.

Steady-state absorbance and fluorescence spectra of blends, transient absorption decays as a function intensity, kinetic fits and details of modeling (PDF)

■ AUTHOR INFORMATION

Corresponding Authors

*stoichko.dimitrov@swansea.ac.uk

*jenny.nelson@imperial.ac.uk

ORCID

S. D. Dimitrov: 0000-0002-1564-7080

M. Azzouzi: 0000-0001-5190-9984

I. McCulloch: 0000-0002-6340-7217

J. R. Durrant: 0000-0001-8353-7345

Notes

The authors declare no competing financial interest.

■ ACKNOWLEDGMENTS

This work is part-funded by the European regional Development Fund through the Welsh Government. We thank the EPSRC via grants EP/H040218, EP/I019278, EP/P005543 and EP/M025020 and for a postgraduate studentship for M.A. J.N. thanks the European Research Council for support under the European Union's Horizon 2020 research and innovation program (grant agreement No 742708). B.C.S. would like to acknowledge the British Council (Grant No. 337067). The work at UH was funded in part by the National Science Foundation (CHE-1664971) and the Robert A. Welch Foundation (E-1337).

■ REFERENCES

(1) Meng, L.; Zhang, Y.; Wan, X.; Li, C.; Zhang, X.; Wang, Y.; Ke, X.; Xiao, Z.; Ding, L.; Xia, R.; et al. Organic and Solution-Processed Tandem Solar Cells with 17.3% Efficiency. *Science (Washington, DC, U. S.)* **2018**, *361* (6407), 1094−1098.

(2) Banerji, N. Pushing the Knowledge of Interfaces. *Nat. Mater.* **2017**, *16*, 503.

(3) Zhang, J.; Jakowetz, A. C.; Li, G.; Di, D.; Menke, S. M.; Rao, A.; Friend, R. H.; Bakulin, A. A. On the Energetics of Bound Charge-Transfer States in Organic Photovoltaics. *J. Mater. Chem. A* **2017**, *5* (23), 11949−11959.

(4) Bakulin, A. A.; Rao, A.; Pavelyev, V. G.; van Loosdrecht, P. H. M.; Pshenichnikov, M. S.; Niedzialek, D.; Cornil, J.; Beljonne, D.; Friend, R. H. The Role of Driving Energy and Delocalized States for Charge Separation in Organic Semiconductors. *Science (Washington, DC, U. S.)* **2012**, *335* (6074), 1340−1344.

(5) Albrecht, S.; Vandewal, K.; Tumbleston, J. R.; Fischer, F. S. U.; Douglas, J. D.; Fréchet, J. M. J.; Ludwigs, S.; Ade, H.; Salleo, A.; Neher, D. On the Efficiency of Charge Transfer State Splitting in Polymer:Fullerene Solar Cells. *Adv. Mater.* **2014**, *26* (16), 2533−2539.

(6) Vandewal, K.; Albrecht, S.; Hoke, E. T.; Graham, K. R.; Widmer, J.; Douglas, J. D.; Schubert, M.; Mateker, W. R.; Bloking, J. T.; Burkhard, G. F.; et al. Efficient Charge Generation by Relaxed Charge-Transfer States at Organic Interfaces. *Nat. Mater.* **2014**, *13*, 63.

(7) Ohkita, H.; Cook, S.; Astuti, Y.; Duffy, W.; Tierney, S.; Zhang, W.; Heeney, M.; McCulloch, I.; Nelson, J.; Bradley, D. D. C.; et al. Charge Carrier Formation in Polythiophene/Fullerene Blend Films Studied by Transient Absorption Spectroscopy. *J. Am. Chem. Soc.* **2008**, *130* (10), 3030−3042.

(8) Lee, J.; Vandewal, K.; Yost, S. R.; Bahlke, M. E.; Goris, L.; Baldo, M. A.; Manca, J. V.; Van Voorhis, T. Charge Transfer State Versus Hot Exciton Dissociation in Polymer−Fullerene Blended Solar Cells. *J. Am. Chem. Soc.* **2010**, *132* (34), 11878−11880.

(9) Clarke, T. M.; Peet, J.; Lungenschmied, C.; Drolet, N.; Lu, X.; Ocko, B. M.; Mozer, A. J.; Loi, M. A. The Role of Emissive Charge Transfer States in Two Polymer-Fullerene Organic Photovoltaic Blends: Tuning Charge Photogeneration through the Use of Processing Additives. *J. Mater. Chem. A* **2014**, *2* (31), 12583−12593.

(10) Barker, A. J.; Chen, K.; Hodgkiss, J. M. Distance Distributions of Photogenerated Charge Pairs in Organic Photovoltaic Cells. *J. Am. Chem. Soc.* **2014**, *136* (34), 12018−12026.

(11) Piliego, C.; Loi, M. A. Charge Transfer State in Highly Efficient Polymer-Fullerene Bulk Heterojunction Solar Cells. *J. Mater. Chem.* **2012**, *22* (10), 4141−4150.

(12) Hallermann, M.; Kriegel, I.; Da Como, E.; Berger, J. M.; von Hauff, E.; Feldmann, J. Charge Transfer Excitons in Polymer/Fullerene Blends: The Role of Morphology and Polymer Chain Conformation. *Adv. Funct. Mater.* **2009**, *19* (22), 3662−3668.

(13) Etzold, F.; Howard, I. A.; Forler, N.; Cho, D. M.; Meister, M.; Mangold, H.; Shu, J.; Hansen, M. R.; Müllen, K.; Laquai, F. The Effect of Solvent Additives on Morphology and Excited-State Dynamics in PCPDTBT:PCBM Photovoltaic Blends. *J. Am. Chem. Soc.* **2012**, *134* (25), 10569−10583.

(14) Albrecht, S.; Schindler, W.; Kurpiers, J.; Kniepert, J.; Blakesley, J. C.; Dumsch, I.; Allard, S.; Fostiropoulos, K.; Scherf, U.; Neher, D. On the Field Dependence of Free Charge Carrier Generation and Recombination in Blends of PCPDTBT/PC70BM: Influence of Solvent Additives. *J. Phys. Chem. Lett.* **2012**, *3* (5), 640−645.

(15) Tvingstedt, K.; Vandewal, K.; Zhang, F.; Inganäs, O. On the Dissociation Efficiency of Charge Transfer Excitons and Frenkel Excitons in Organic Solar Cells: A Luminescence Quenching Study. *J. Phys. Chem. C* **2010**, *114* (49), 21824−21832.

(16) Dimitrov, S. D.; Wheeler, S.; Niedzialek, D.; Schroeder, B. C.; Utzat, H.; Frost, J. M.; Yao, J.; Gillett, A.; Tuladhar, P. S.; McCulloch, I.; et al. Polaron Pair Mediated Triplet Generation in Polymer/fullerene Blends. *Nat. Commun.* **2015**, *6*, 6501.

(17) Zhou, Y.; Tvingstedt, K.; Zhang, F.; Du, C.; Ni, W.-X.; Andersson, M. R.; Inganäs, O. Observation of a Charge Transfer State in Low-Bandgap Polymer/Fullerene Blend Systems by Photoluminescence and Electroluminescence Studies. *Adv. Funct. Mater.* **2009**, *19* (20), 3293−3299.

(18) Veldman, D.; İpek, Ö.; Meskers, S. C. J.; Sweelssen, J.; Koetse, M. M.; Veenstra, S. C.; Kroon, J. M.; van Bavel, S. S.; Loos, J.; Janssen, R. A. J. Compositional and Electric Field Dependence of the Dissociation of Charge Transfer Excitons in Alternating Polyfluorene Copolymer/Fullerene Blends. *J. Am. Chem. Soc.* **2008**, *130* (24), 7721−7735.

(19) Dimitrov, S. D.; Bakulin, A. A.; Nielsen, C. B.; Schroeder, B. C.; Du, J.; Bronstein, H.; McCulloch, I.; Friend, R. H.; Durrant, J. R. On the Energetic Dependence of Charge Separation in Low-Band-Gap Polymer/fullerene Blends. *J. Am. Chem. Soc.* **2012**, *134* (44), 18189−18192.

(20) Bakulin, A. A.; Dimitrov, S. D.; Rao, A.; Chow, P. C. Y.; Nielsen, C. B.; Schroeder, B. C.; McCulloch, I.; Bakker, H. J.; Durrant, J. R.; Friend, R. H. Charge-Transfer State Dynamics Following Hole and Electron Transfer in Organic Photovoltaic Devices. *J. Phys. Chem. Lett.* **2013**, *4* (1), 209−215.

(21) Coffey, D. C.; Larson, B. W.; Hains, A. W.; Whitaker, J. B.; Kopidakis, N.; Boltalina, O. V.; Strauss, S. H.; Rumbles, G. An Optimal Driving Force for Converting Excitons into Free Carriers in Excitonic Solar Cells. *J. Phys. Chem. C* **2012**, *116* (16), 8916−8923.

(22) Wang, T.; Kafle, T. R.; Kattel, B.; Chan, W.-L. A Multidimensional View of Charge Transfer Excitons at Organic Donor−Acceptor Interfaces. *J. Am. Chem. Soc.* **2017**, *139* (11), 4098−4106.

(23) Armin, A.; Zhang, Y.; Burn, P. L.; Meredith, P.; Pivrikas, A. Measuring Internal Quantum Efficiency to Demonstrate Hot Exciton Dissociation. *Nat. Mater.* **2013**, *12*, 593.
(24) Armin, A.; Kassal, I.; Shaw, P. E.; Hambsch, M.; Stolterfoht, M.; Lyons, D. M.; Li, J.; Shi, Z.; Burn, P. L.; Meredith, P. Spectral Dependence of the Internal Quantum Efficiency of Organic Solar Cells: Effect of Charge Generation Pathways. *J. Am. Chem. Soc.* **2014**, *136* (32), 11465−11472.
(25) Menke, S. M.; Cheminal, A.; Conaghan, P.; Ran, N. A.; Greehnam, N. C.; Bazan, G. C.; Nguyen, T.-Q.; Rao, A.; Friend, R. H. Order Enables Efficient Electron-Hole Separation at an Organic Heterojunction with a Small Energy Loss. *Nat. Commun.* **2018**, *9* (1), 277.
(26) Bittner, E. R.; Silva, C. Noise-Induced Quantum Coherence Drives Photo-Carrier Generation Dynamics at Polymeric Semiconductor Heterojunctions. *Nat. Commun.* **2014**, *5*, 3119.
(27) Collins, B. A.; Li, Z.; Tumbleston, J. R.; Gann, E.; McNeill, C. R.; Ade, H. Absolute Measurement of Domain Composition and Nanoscale Size Distribution Explains Performance in PTB7:PC71BM Solar Cells. *Adv. Energy Mater.* **2013**, *3* (1), 65−74.
(28) Martens, T.; D'Haen, J.; Munters, T.; Beelen, Z.; Goris, L.; Manca, J.; D'Olieslaeger, M.; Vanderzande, D.; De Schepper, L.; Andriessen, R. Disclosure of the Nanostructure of MDMO-PPV:PCBM Bulk Hetero-Junction Organic Solar Cells by a Combination of SPM and TEM. *Synth. Met.* **2003**, *138* (1), 243−247.
(29) Pearson, A. J.; Wang, T.; Dunbar, A. D. F.; Yi, H.; Watters, D. C.; Coles, D. M.; Staniec, P. A.; Iraqi, A.; Jones, R. A. L.; Lidzey, D. G. Morphology Development in Amorphous Polymer:Fullerene Photovoltaic Blend Films During Solution Casting. *Adv. Funct. Mater.* **2014**, *24* (5), 659−667.
(30) Jamieson, F. C.; Domingo, E. B.; McCarthy-Ward, T.; Heeney, M.; Stingelin, N.; Durrant, J. R. Fullerene Crystallisation as a Key Driver of Charge Separation in Polymer/fullerene Bulk Heterojunction Solar Cells. *Chem. Sci.* **2012**, *3* (2), 485−492.
(31) Mayer, A. C.; Toney, M. F.; Scully, S. R.; Rivnay, J.; Brabec, C. J.; Scharber, M.; Koppe, M.; Heeney, M.; McCulloch, I.; McGehee, M. D. Bimolecular Crystals of Fullerenes in Conjugated Polymers and the Implications of Molecular Mixing for Solar Cells. *Adv. Funct. Mater.* **2009**, *19*, 1173−1179.
(32) Utzat, H.; Dimitrov, S. D.; Wheeler, S.; Collado-Fregoso, E.; Tuladhar, P. S.; Schroeder, B. C.; McCulloch, I.; Durrant, J. R. Charge Separation in Intermixed polymer:PC70BM Photovoltaic Blends: Correlating Structural and Photophysical Length Scales as a Function of Blend Composition. *J. Phys. Chem. C* **2017**, *121* (18), 9790−9801.
(33) Causa', M.; De Jonghe-Risse, J.; Scarongella, M.; Brauer, J. C.; Buchaca-Domingo, E.; Moser, J.-E.; Stingelin, N.; Banerji, N. The Fate of Electron−hole Pairs in Polymer:fullerene Blends for Organic Photovoltaics. *Nat. Commun.* **2016**, *7*, 12556.
(34) Gehrig, D. W.; Howard, I. A.; Sweetnam, S.; Burke, T. M.; McGehee, M. D.; Laquai, F. The Impact of Donor−Acceptor Phase Separation on the Charge Carrier Dynamics in pBTTT:PCBM Photovoltaic Blends. *Macromol. Rapid Commun.* **2015**, *36* (11), 1054−1060.
(35) Faist, M. A.; Shoaee, S.; Tuladhar, S.; Dibb, G. F. A.; Foster, S.; Gong, W.; Kirchartz, T.; Bradley, D. D. C.; Durrant, J. R.; Nelson, J. Understanding the Reduced Efficiencies of Organic Solar Cells Employing Fullerene Multiadducts as Acceptors. *Adv. Energy Mater.* **2013**, *3* (6), 744−752.
(36) Jakowetz, A. C.; Böhm, M. L.; Zhang, J.; Sadhanala, A.; Huettner, S.; Bakulin, A. A.; Rao, A.; Friend, R. H. What Controls the Rate of Ultrafast Charge Transfer and Charge Separation Efficiency in Organic Photovoltaic Blends. *J. Am. Chem. Soc.* **2016**, *138* (36), 11672−11679.
(37) Dimitrov, S. D.; Nielsen, C. B.; Shoaee, S.; Shakya Tuladhar, P.; Du, J.; McCulloch, I.; Durrant, J. R. Efficient Charge Photogeneration by the Dissociation of PC 70BM Excitons in Polymer/fullerene Solar Cells. *J. Phys. Chem. Lett.* **2012**, *3* (1), 140−144.
(38) Dibb, G. F. A.; Jamieson, F. C.; Maurano, A.; Nelson, J.; Durrant, J. R. Limits on the Fill Factor in Organic Photovoltaics: Distinguishing Nongeminate and Geminate Recombination Mechanisms. *J. Phys. Chem. Lett.* **2013**, *4* (5), 803−808.
(39) Baran, D.; Li, N.; Breton, A.-C.; Osvet, A.; Ameri, T.; Leclerc, M.; Brabec, C. J. Qualitative Analysis of Bulk-Heterojunction Solar Cells without Device Fabrication: An Elegant and Contactless Method. *J. Am. Chem. Soc.* **2014**, *136* (31), 10949−10955.
(40) Faist, M. A. *Spectroscopic Studies of the Charge Transfer State and Device Performance of Polymer:Fullerene Photovoltaic Blends*; Imperial College London, 2012.
(41) Guilbert, A. A. Y.; Schmidt, M.; Bruno, A.; Yao, J.; King, S.; Tuladhar, S. M.; Kirchartz, T.; Alonso, M. I.; Goñi, A. R.; Stingelin, N.; et al. Spectroscopic Evaluation of Mixing and Crystallinity of Fullerenes in Bulk Heterojunctions. *Adv. Funct. Mater.* **2014**, *24* (44), 6972−6980.
(42) Kästner, C.; Vandewal, K.; Egbe, D. A. M.; Hoppe, H. Revelation of Interfacial Energetics in Organic Multiheterojunctions. *Adv. Sci.* **2017**, *4* (4), 1600331.
(43) Rao, A.; Chow, P. C. Y.; Gelinas, S.; Schlenker, C. W.; Li, C.-Z.; Yip, H.-L.; Jen, A. K.-Y.; Ginger, D. S.; Friend, R. H. The Role of Spin in the Kinetic Control of Recombination in Organic Photovoltaics. *Nature* **2013**, *500* (7463), 435−439.
(44) Schroeder, B. C.; Huang, Z.; Ashraf, R. S.; Smith, J.; D'Angelo, P.; Watkins, S. E.; Anthopoulos, T. D.; Durrant, J. R.; McCulloch, I. Silaindacenodithiophene-Based Low Band Gap Polymers - The Effect of Fluorine Substitution on Device Performances and Film Morphologies. *Adv. Funct. Mater.* **2012**, *22*, 1663−1670.
(45) Etzold, F.; Howard, I. A.; Mauer, R.; Meister, M.; Kim, T.-D.; Lee, K.-S.; Baek, N. S.; Laquai, F. Ultrafast Exciton Dissociation Followed by Nongeminate Charge Recombination in PCDTBT:PCBM Photovoltaic Blends. *J. Am. Chem. Soc.* **2011**, *133* (24), 9469−9479.
(46) Stolterfoht, M.; Shoaee, S.; Armin, A.; Jin, H.; Kassal, I.; Jiang, W.; Burn, P.; Meredith, P. Electric Field and Mobility Dependent First-Order Recombination Losses in Organic Solar Cells. *Adv. Energy Mater.* **2017**, *7* (4), 1601379.
(47) Collado-Fregoso, E.; Deledalle, F.; Utzat, H.; Tuladhar, P. S.; Dimitrov, S. D.; Gillett, A.; Tan, C. H.; Zhang, W.; McCulloch, I.; Durrant, J. R. Photophysical Study of DPPTT-T/PC70BM Blends and Solar Devices as a Function of Fullerene Loading: An Insight into EQE Limitations of DPP-Based Polymers. *Adv. Funct. Mater.* **2017**, *27* (6), 1604426.
(48) Di Nuzzo, D.; Koster, L. J. A.; Gevaerts, V. S.; Meskers, S. C. J.; Janssen, R. A. J. The Role of Photon Energy in Free Charge Generation in Bulk Heterojunction Solar Cells. *Adv. Energy Mater.* **2014**, *4* (18), 1400416.
(49) Melianas, A.; Etzold, F.; Savenije, T. J.; Laquai, F.; Inganäs, O.; Kemerink, M. Photo-Generated Carriers Lose Energy during Extraction from Polymer-Fullerene Solar Cells. *Nat. Commun.* **2015**, *6*, 8778.
(50) Peng, Z.; Jiao, X.; Ye, L.; Li, S.; Rech, J. J.; You, W.; Hou, J.; Ade, H. Measuring Temperature-Dependent Miscibility for Polymer Solar Cell Blends: An Easily Accessible Optical Method Reveals Complex Behavior. *Chem. Mater.* **2018**, *30* (12), 3943−3951.
(51) Ma, W.; Tumbleston, J. R.; Wang, M.; Gann, E.; Huang, F.; Ade, H. Domain Purity, Miscibility, and Molecular Orientation at Donor/Acceptor Interfaces in High Performance Organic Solar Cells: Paths to Further Improvement. *Adv. Energy Mater.* **2013**, *3* (7), 864−872.
(52) Collins, B. A.; Gann, E.; Guignard, L.; He, X.; McNeill, C. R.; Ade, H. Molecular Miscibility of Polymer−Fullerene Blends. *J. Phys. Chem. Lett.* **2010**, *1* (21), 3160−3166.
(53) Ye, L.; Hu, H.; Ghasemi, M.; Wang, T.; Collins, B. A.; Kim, J.-H.; Jiang, K.; Carpenter, J. H.; Li, H.; Li, Z.; et al. Quantitative Relations between Interaction Parameter, Miscibility and Function in Organic Solar Cells. *Nat. Mater.* **2018**, *17* (3), 253−260.
(54) Kurpiers, J.; Ferron, T.; Roland, S.; Jakoby, M.; Thiede, T.; Jaiser, F.; Albrecht, S.; Janietz, S.; Collins, B. A.; Howard, I. A.; et al. Probing the Pathways of Free Charge Generation in Organic Bulk Heterojunction Solar Cells. *Nat. Commun.* **2018**, *9* (1), 2038.

DOI: 10.1021/jacs.8b11484
J. Am. Chem. Soc. 2019, 141, 4634−4643

(55) Karabunarliev, S.; Bittner, E. R. Dissipative Dynamics of Spin-Dependent Electron−hole Capture in Conjugated Polymers. *J. Chem. Phys.* **2003**, *119* (7), 3988−3995.
(56) Karabunarliev, S.; Bittner, E. R. Polaron−excitons and Electron−vibrational Band Shapes in Conjugated Polymers. *J. Chem. Phys.* **2003**, *118* (9), 4291−4296.
(57) Karabunarliev, S.; Bittner, E. R. Spin-Dependent Electron-Hole Capture Kinetics in Luminescent Conjugated Polymers. *Phys. Rev. Lett.* **2003**, *90* (5), 57402.
(58) Savoie, B. M.; Rao, A.; Bakulin, A. A.; Gelinas, S.; Movaghar, B.; Friend, R. H.; Marks, T. J.; Ratner, M. A. Unequal Partnership: Asymmetric Roles of Polymeric Donor and Fullerene Acceptor in Generating Free Charge. *J. Am. Chem. Soc.* **2014**, *136* (7), 2876−2884.
(59) Kahle, F.-J.; Saller, C.; Olthof, S.; Li, C.; Lebert, J.; Weiß, S.; Herzig, E. M.; Hüttner, S.; Meerholz, K.; Strohriegl, P.; et al. Does Electron Delocalization Influence Charge Separation at Donor−Acceptor Interfaces in Organic Photovoltaic Cells? *J. Phys. Chem. C* **2018**, *122* (38), 21792−21802.
(60) Burke, T. M.; McGehee, M. D. How High Local Charge Carrier Mobility and an Energy Cascade in a Three-Phase Bulk Heterojunction Enable > 90% Quantum Efficiency. *Adv. Mater.* **2014**, *26* (12), 1923−1928.

DOI: 10.1021/jacs.8b11484
J. Am. Chem. Soc. 2019, 141, 4634−4643